Joule

CellPress

Article

Angle-selective thermal emitter for directional radiative cooling and heating

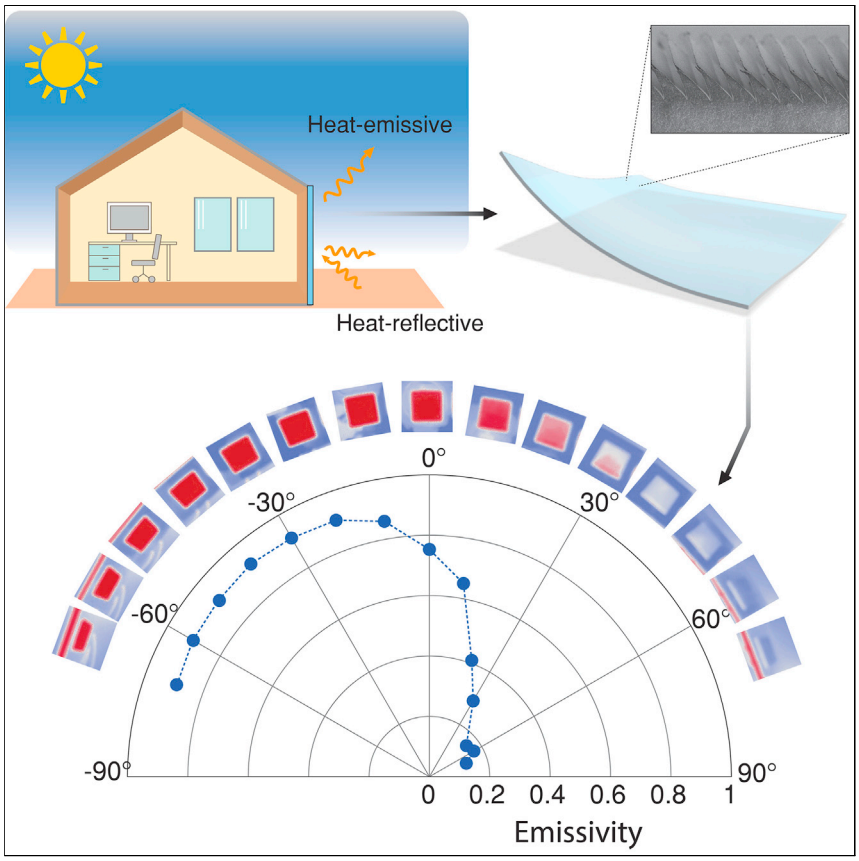

Changing how materials emit heat can help save energy in buildings. Such examples include low-emissivity windows and radiatively cooling paints. The past strategies have mostly focused on the spectral properties of radiated heat, whereas changing the direction of radiated heat can bring further energy-saving benefits. We demonstrate a flexible, micro-structured film capable of emitting heat in specific directions. This material allows us to achieve energy savings compared with conventional isotropic emitters, especially in scenarios where environmental temperatures are inhomogeneous, for example, in outdoor radiative cooling for building walls or heating specific areas indoors.

Jiawei Zhou, Tony G. Chen, Yoichiro Tsurimaki, ..., Shanhui Fan, Mark R. Cutkosky, Yi Cui

yicui@stanford.edu

Highlights

Tilted-wedge surface microstructures enable broadband tuning of directional emissivity

Angle-selective emitters allow directional radiative cooling to the sky

Directional emitters enhance local heat radiation for higher energy efficiency

Zhou et al., Joule 7, 1–15
December 20, 2023
https://doi.org/10.1016/j.joule.2023.10.013

Please cite this article in press as: Zhou et al., Angle-selective thermal emitter for directional radiative cooling and heating, Joule (2023), https://doi.org/10.1016/j.joule.2023.10.013

Joule

CellPress

Article

Angle-selective thermal emitter for directional radiative cooling and heating

Jiawei Zhou,[1,6] Tony G. Chen,[2,6] Yoichiro Tsurimaki,[3] Amar Hajj-Ahmad,[2] Lingling Fan,[3] Yucan Peng,[1] Rong Xu,[1] Yecun Wu,[3] Sid Assawaworrarit,[3] Shanhui Fan,[3] Mark R. Cutkosky,[2] and Yi Cui[1,4,5,7,*]

SUMMARY

Material emissivity engineering can boost energy efficiency in cooling and heating systems by tailoring radiative heat exchange. However, practical energy saving often faces challenges due to environmental temperature inhomogeneity, such as building walls encountering both cold sky and hot ground in the summer. Matching the inhomogeneous temperature requires angle-selective emissivity materials. We present a micro-wedge structure for directional thermal emission control. Our design shows a large broadband contrast in directional emissivity (0.9–0.1), with the angular emission range controlled by the micro-wedge geometry and tunable through magnetic coupling. The angle-selective emitter offers better daytime radiative cooling for outdoor vertical surfaces (2°C below isotropic emitters), potentially saving 10%–40% cooling energy, and efficient indoor radiant heating. Harnessing the directional characteristic of thermal emission opens new opportunities in energy efficiency enhancements across various applications, such as space heating and cooling, waste heat recovery, and solar thermal power generation.

INTRODUCTION

Cooling and heating are responsible for over one-third of global energy-related greenhouse gas emissions.[1] The regulation of heat exchange is pivotal in achieving energy-efficient cooling and heating, and one effective strategy is to tailor heat radiation through engineering the spectral emissivity of materials.[2–6] In the building sector, low-emissivity glass reduces the thermal conductance in glazing units, minimizing heat loss to the environment and helping to maintain indoor comfort throughout the year.[3] Low-emissivity paints, when applied to non-transparent building surfaces, diminish heat absorption from the sun and surroundings during summer while limiting radiative heat loss in winter.[7] On the contrary, high-emissivity materials allow heat to be efficiently dissipated into the environment through radiation.[8] Passive daytime radiative cooling has emerged as a strategy to cool objects including buildings by designing materials with high solar reflectivity and high infrared emissivity in the atmospheric transparency window at 8–13 μm.[9–15] In recent years, spectral emissivity engineering has also emerged for personal thermal management, where advanced textile materials are designed to transmit or reflect thermal radiation from the human body to facilitate personal thermal comfort.[16–19]

Although engineering spectral emissivity is effective when the surrounding environment is at homogeneous and steady temperatures, the environment's temperatures are largely inhomogeneous and can dynamically vary in many practical situations.[20]

CONTEXT & SCALE

Thermal emission is a fundamental phenomenon of nature with impacts on various energy technologies. Spectral thermal emissivity engineering has led to innovative designs that improve heating and cooling energy efficiency, including low-emissivity windows, radiatively cooling paints, and personal cooling textiles. Directional control of thermal emission can unlock new possibilities in thermal technologies, which however requires scalable materials with large broadband emissivity contrast. We developed a flexible thin film material with significant changes in the emissivity at different angles. These angle-selective emitters offer advantages over conventional materials for energy-saving applications, including radiative cooling in outdoor environments and indoor space heating. Our research represents a new approach to thermal management with the potential to enhance various thermal technologies, including space heating and cooling, solar thermal power generation, and waste heat recovery.

Please cite this article in press as: Zhou et al., Angle-selective thermal emitter for directional radiative cooling and heating, Joule (2023), https://doi.org/10.1016/j.joule.2023.10.013

Take the residential building as an example. During summer, while the sky stays cold, the ground temperature rises significantly due to solar heat gain (Figure 1A). Efficient cooling of the building walls to promote energy efficiency therefore calls for materials with directional infrared emissivity—able to simultaneously radiate to cold sources (e.g., by having high emissivity toward the sky) while reflecting heat from the hot environments (e.g., by having low emissivity toward the ground). The indoor environment exhibits large temperature inhomogeneity as well,[2] particularly between human bodies and other indoor items (Figure 1A). Radiant heaters—indoor heating panels that transfer heat through radiation[21]—can consume less energy by directing radiative heat only to a target. Moreover, materials with adaptive directional emissivity can further optimize cooling and heating energy efficiency in response to changing weather conditions and moving targets.

Although spectral engineering of thermal emissivity has been extensively achieved through the thermal photonic approach,[8,9] directional engineering is less frequently reported,[22–24] and is particularly challenging for thermal emission as the latter is a broadband phenomenon that spans a wide range of wavelengths.[25,26] Exploiting the direction of heat radiation to achieve energy savings for heating and cooling further sets a stringent requirement on the emissivity profiles because the emissivity needs to be close to one in the direction where radiative energy exchange is desired, whereas being close to zero in the direction where such energy exchange is unwanted. In addition, the high-emissivity direction oftentimes needs to be asymmetric with respect to the normal incidence direction to meet practical requirements (e.g., radiative cooling for building walls), which indicates that symmetric grating or multilayer structures would not suffice. In this work, we propose a microstructure design that achieves asymmetric angle-selective thermal emissivity, with large contrast in spectral directional emissivity varying from 0.9 to 0.1 as a function of angles. This material adapts its directional emissivity to the large temperature inhomogeneity in the environment for radiative cooling, realizing simultaneous heat dissipation to cold sources and rejection of heat from a hot environment. We also demonstrate that angle-selective emission can deliver radiative energy to a target and achieves energy saving for radiant heating. The angular range of thermal emission can be further tuned using magnetically responsive soft materials, making directional emitters adaptable to dynamically varying environments.

RESULTS

Design of angle-selective thermal emitter

Kirchhoff's law of thermal radiation indicates that directional spectral emissivity ε and absorptivity α at a given direction and wavelength are identical, namely, $\varepsilon(\theta,\lambda) = \alpha(\theta, \lambda)$. Designing materials with angle-selective emissivity thus translates to finding structures with strong absorption only at certain angles. Here, we design microstructures that promote absorption within a selective range of angles. The proposed structure is composed of periodically placed tilted wedges made of polydimethylsiloxane (PDMS; see Figure 1B), about the same order of magnitude with the peak thermal radiation wavelength at room temperature (about 10 μm). The top surface of the wedges is further coated with aluminum. PDMS has an intrinsic high absorptivity/emissivity about 0.9 near 10 μm, whereas aluminum has an emissivity typically less than 0.1 in the mid-infrared range and can reflect most of infrared radiation. When incident radiation comes at an angle facing the wedges, significant electromagnetic energy enters the space between the wedges, leading to strong absorption of thermal radiation, as demonstrated by local enhancement of the electromagnetic fields (Figure 1C). On the contrary, if incident radiation comes at angles facing

[1]Department of Materials Science and Engineering, Stanford University, Stanford, CA 94305, USA

[2]Department of Mechanical Engineering, Stanford University, Stanford, CA 94305, USA

[3]Department of Electrical Engineering, Stanford University, Stanford, CA 94305, USA

[4]Department of Energy Science and Engineering, Stanford University, Stanford, CA 94305, USA

[5]Stanford Institute for Materials and Energy Sciences, SLAC National Accelerator Laboratory, Menlo Park, CA 94025, USA

[6]These authors contributed equally

[7]Lead contact

*Correspondence: yicui@stanford.edu

https://doi.org/10.1016/j.joule.2023.10.013

Please cite this article in press as: Zhou et al., Angle-selective thermal emitter for directional radiative cooling and heating, Joule (2023), https://doi.org/10.1016/j.joule.2023.10.013

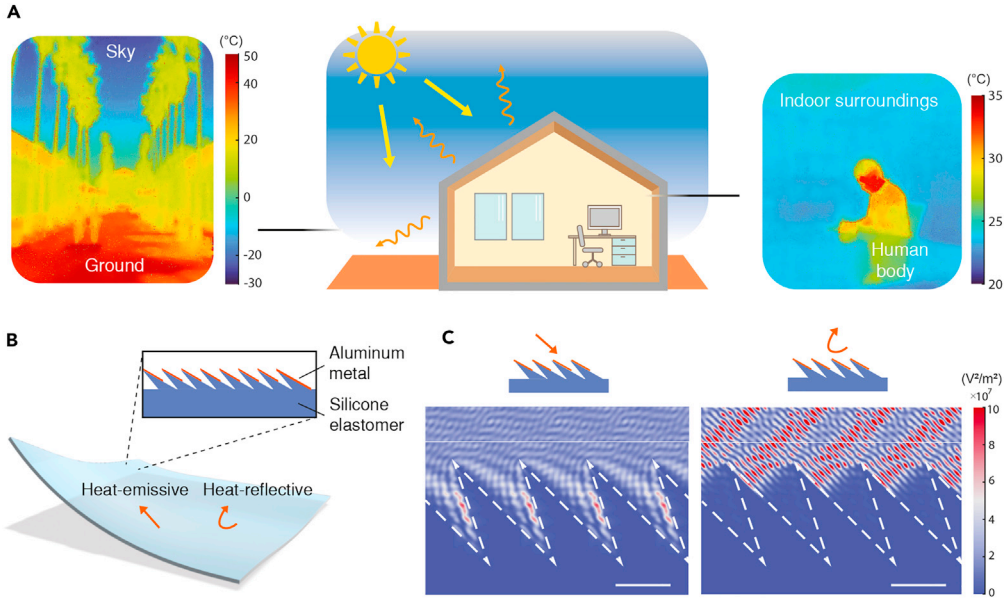

Figure 1. Concept of angle-selective thermal emitter

(A) Schematic of the typical environment of a residential building. Infrared images of both outdoor and indoor environments display large temperature inhomogeneity.

(B) Proposed structure to achieve angle-selective thermal emissivity, utilizing microstructures to enhance radiative absorption (and thus emission) in one direction while promoting reflection in the other direction.

(C) Simulated electromagnetic field profiles for waves with transverse electric field polarization at different incidence angles. The color bars indicate the square of the electric field magnitude. The wavelength of the incoming wave is 10 μm, and the incident power density is 1 W/m. The scale bar represents 50 μm.

the aluminum-coated surfaces, most radiative heat is reflected (Figure 1C). The strong absorption in one direction but not the other thereby leads to an angle-dependent thermal emissivity.

To fabricate the structure, we used a scalable approach based on computer numerical control (CNC) molding, casting, and metal deposition (Figure 2A; experimental procedures). Briefly, a wax mold is first created using a hybrid process of orthogonal cutting and wedge indenting[27] with a sharp microtome blade (~1 μm tip radius). A series of indentations is made on the surface of the wax mold to create wedge-shaped cavities on the order of 100 μm. The angle, depth, and spacing of these wedges can be controlled by adjusting the tool geometry and the machining path. A two-part silicone is then poured into the mold to create a PDMS film with micro-wedge structures. The resulting film peeled off from the mold is soft and stretchable with a thickness around 150 μm (Figures 2B and S1), making it adaptable to different geometries and shapes. The surface of the PDMS film is further plasma cleaned and subsequently deposited with aluminum metal (150-nm thickness). Scanning electron microscopy of the cross-section shows that the wedges have sharp ends that are beneficial for trapping heat radiation (Figure 2C).

To quantify the angle-dependent thermal emissivity, we used a Fourier transform infrared spectrometer to measure the emissivity spectrum (see details in experimental procedures and Figure S2). Figure 2D shows the measured spectral directional emissivity of emitter sample 1 at selected angles, together with corresponding infrared images taken when the sample is placed on a heater. Here, the angle is defined as the polar angle varying in the same plane as the wedge structure (see inset

Please cite this article in press as: Zhou et al., Angle-selective thermal emitter for directional radiative cooling and heating, Joule (2023), https://doi.org/10.1016/j.joule.2023.10.013

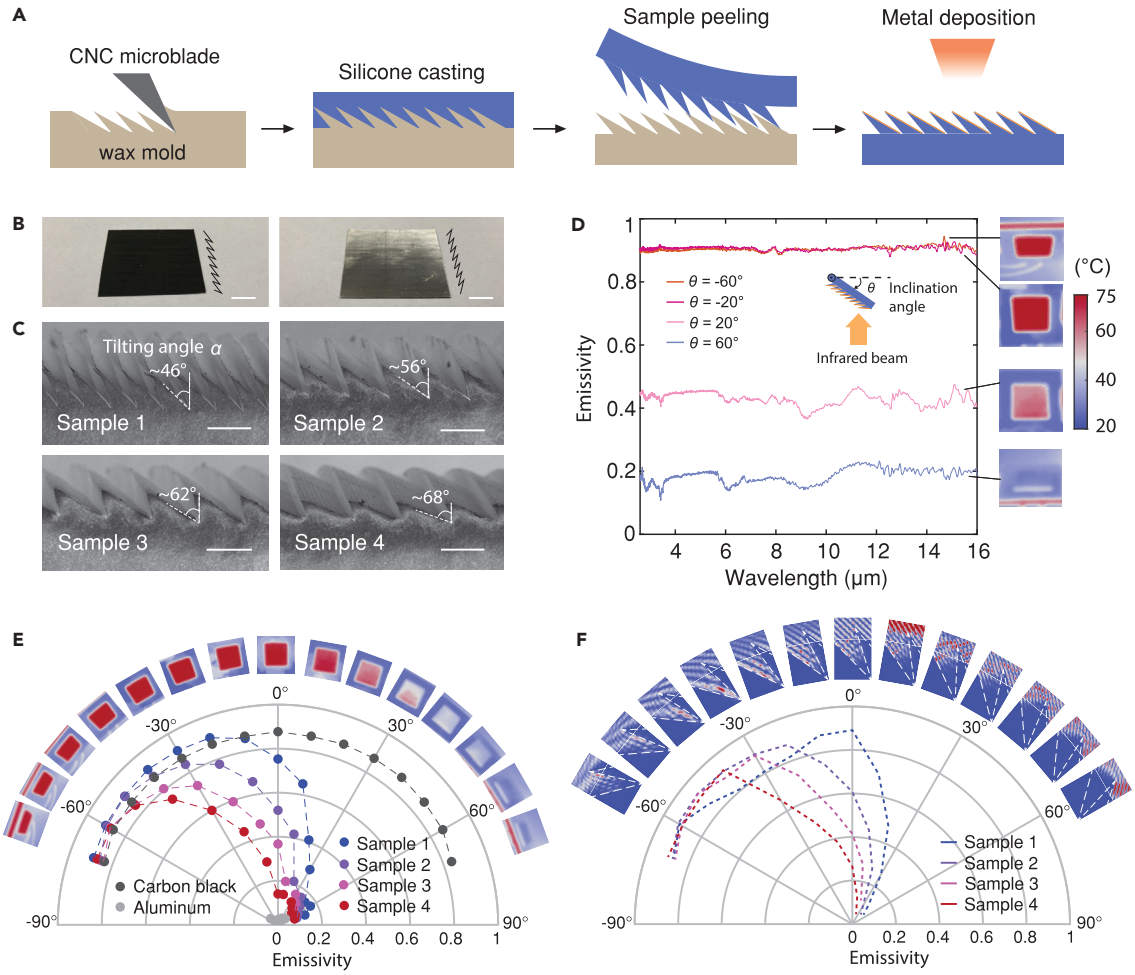

Figure 2. Fabrication and characterization of angle-selective thermal emitter

(A) Schematic of the fabrication process of the angle-selective thermal emitter.

(B) Photos of a directional thermal emitter material from different viewing angles. The scale bar represents 1 cm.

(C) Scanning electron microscopy images of cross sections of directional emitters with different wedge geometries, labeled as samples 1–4. The scale bar represents 100 μm.

(D) Emissivity spectrum of emitter sample 1 at different incidence angles.

(E) Measured angle-dependent emissivity at the incident wavelength of 10 μm for samples 1–4 with different wedge tilting angles. The pictures on the top show the infrared images taken at different angles for sample 1 (placed on a heater). Carbon black and aluminum mylar as reference materials are also measured, showing no angle dependence.

(F) Simulated angle-dependent emissivity at 10 μm for emitter with different wedge tilting angles. The pictures on the top show the simulated electromagnetic field profiles for transverse electric field polarization at different angles for sample 1.

of Figure 2D). Our microstructure design achieves a broadband contrast in the emissivity from about 0.9 in one direction to about 0.1 in the other direction. Accordingly, the sample appearance under the infrared camera changes from warm (red color) to cool (blue color). Although PDMS already has high emissivity near 10 μm, the wedge structure further enhances the absorption in the direction when the incident radiation faces the wedges, as can be seen by comparing bare PDMS samples with and without wedge structures (Figure S3). This enhancement in absorption (and thus emission) is beneficial to achieve larger radiative energy flux in the direction that is desired. The angular range of high emissivity can be further tuned by wedge geometries. By changing the trajectory of the CNC blade during mold preparation, we can create different shapes that result in wedges with varying tilting angles (Figure 2C, labeled

Please cite this article in press as: Zhou et al., Angle-selective thermal emitter for directional radiative cooling and heating, Joule (2023), https://doi.org/10.1016/j.joule.2023.10.013

as samples 1–4). Our experimental data show that, as the tilting angle of the top surface of the wedge changes from about 46° (sample 1) to about 68° (sample 4), high emissivity is narrowed down into a smaller angular range (Figure 2E; full angle-dependent spectrum data are given in Figures S4 and S5). As a comparison, a commercial carbon black paint shows angle-independent high emissivity, whereas an aluminum mylar film shows low emissivity (Figures 2E and S6). This is corroborated by the electromagnetic wave simulation, which shows measured emissivity at 10 μm for incidence angles from −70° to 70° for four different wedge geometries (Figure 2F; see also Figure S7). The experimentally measured angle-dependent emissivity data are smoother compared with simulation results, possibly due to the shape variations from wedge to wedge, as well as the fact that PDMS and deposited aluminum have surface roughness that creates diffuse scatterings. Although the emissivity varies strongly as a function of the polar angle, the emissivity is insensitive to the azimuthal angle, as seen from infrared images taken at different sample orientations (Figure S8).

We have further characterized the durability of the angle-selective emitter material by measuring its angle-dependent emission spectrum after durability tests, including UV exposure, high temperature, and abrasion tests (see more details in Notes S1–S6 and Figure S9). The emitter material is generally stable against UV exposure and high temperature, showing minimal changes in its angle-dependent emission properties. Abrasion will remove the deposited metal layer on the PDMS structure, which strongly affects the emission properties. In practice, an infrared-transparent top layer (e.g., a thin polyethylene [PE] film) can be used to cover the emitter material such that the emission properties are maintained while the emitter is protected against scratch or abrasion. This top layer can simply serve as a protection layer or can have added functionalities (e.g., minimize solar heating in the outdoor application, as we will discuss below).

Directional radiative cooling

Next, we experimentally demonstrate that angle-selective emitters bring enhanced energy-saving potential compared with isotropic emitters when facing large temperature inhomogeneity in the environment. We first discuss cooling applications, taking the side walls of buildings as an example. During summertime, the side walls that reflect thermal radiation from the hot ground reduce heat gain. However, a common approach using shielding materials such as aluminum foil cannot harness the radiative cooling power to the sky as it has low thermal emissivity in all directions and hence does not efficiently emit to the sky, although it can reflect heat radiation from the ground and most of solar flux. For a vertical blackbody surface, the net cooling power to the sky can be on the order of 60 W/m^2 (for surface and ambient temperatures at 300 K, see analysis in Notes S1–S6). Although this value is about half of the cooling power of a horizontal surface, the areas of building walls are large and present significant opportunities for energy savings. Our structure can harness this cooling channel while minimizing heat gain because it has low emissivity toward the ground and can reflect heat while having high emissivity toward the sky and allowing radiative cooling.

Figure 3A shows the outdoor setup for comparing cooling performance of materials with different emissivity profiles (Figure S10). To demonstrate effects of directional infrared emissivity of the directional emitter on cooling, a carbon black paint and an aluminum mylar film are used as references of high and low isotropic emissivity materials, respectively. Based on the angle-dependent emissivity measurements, we estimated that carbon black sample has about 50 W/m^2 cooling power to the

Please cite this article in press as: Zhou et al., Angle-selective thermal emitter for directional radiative cooling and heating, Joule (2023), https://doi.org/10.1016/j.joule.2023.10.013

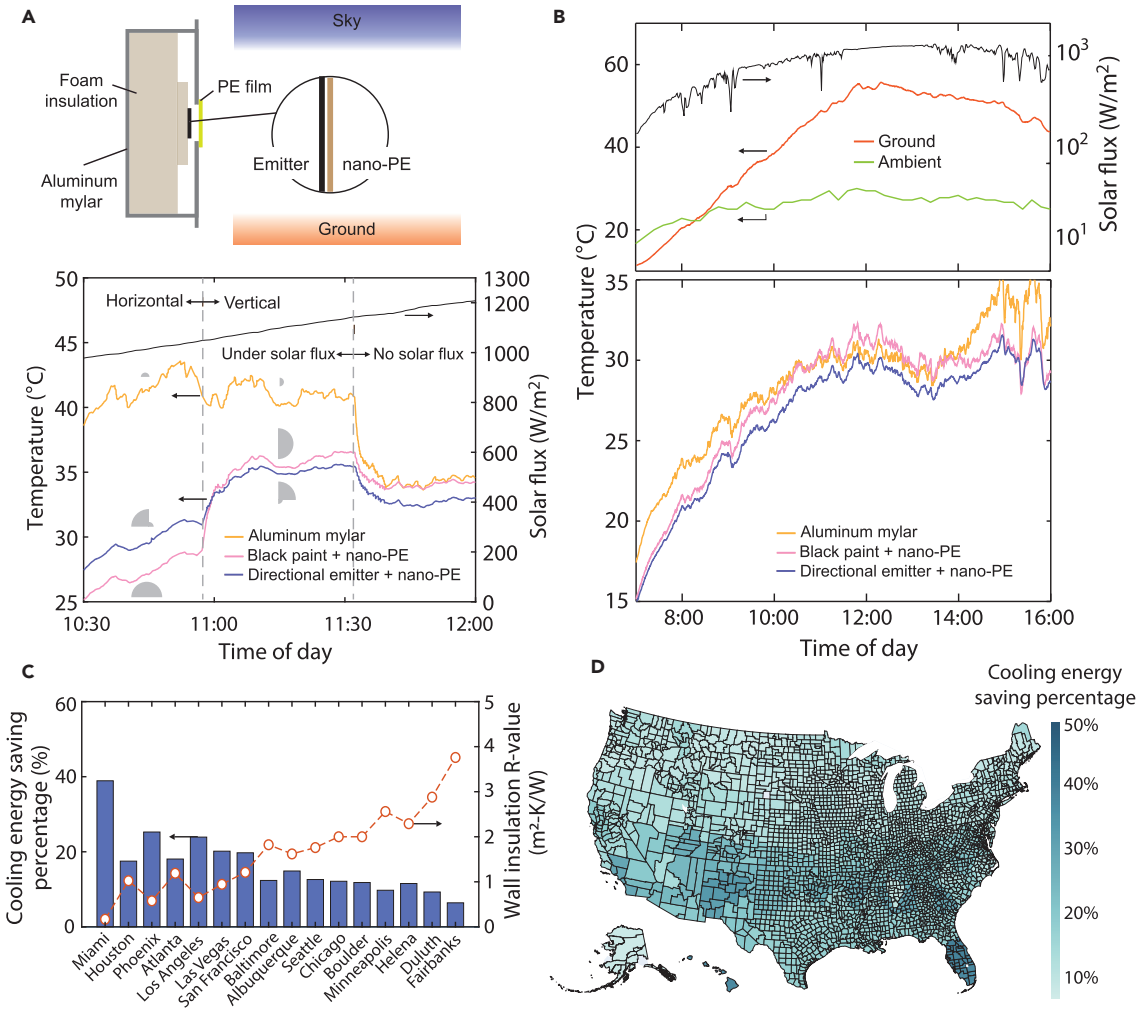

Figure 3. Directional radiative cooling

(A) Orientation test to demonstrate the angle-selective thermal emission property. The top schematic shows the outdoor measurement setup. Polyethylene (PE) film is placed on top of the sample to allow radiative energy exchange while minimizing convective heat loss. For carbon black (blackbody reference) and the directional emitter material (sample 3), an infrared-transparent nano-porous polyethylene (nano-PE) is placed directly on the sample to allow radiative flux to pass through while minimizing solar heat gain. All samples initially are placed horizontally and are then turned vertically, facing both sky and ground.

(B) Full-day outdoor test for vertically installed samples. The top panel shows recorded ground and ambient temperature, as well as solar irradiance. The bottom panel shows the temperature variations of samples with different emissivity profiles.

(C) Cooling energy-saving estimations of 16 representative cities within United States based on heat transfer through building walls.

(D) Energy-saving map within United States.

sky when installed vertically, and directional emitter samples have cooling powers up to 50 W/m^2 depending on wedge angles (Notes S1–S6). To compare the cooling performance of the three materials under similar solar heat gain, the directional emitter and the carbon black surface are further covered with a nano-porous PE (nano-PE) film (about 150 μm thickness) with an average solar reflectance of about 90% and infrared transmittance of about 85% (Figure S10).[28] The high infrared transmittance of nano-PE ensures the infrared emissivity of the emitters is radiatively coupled to the environment, whereas the high solar reflectance rejects most of the solar flux, keeping the solar irradiation on the three materials similar. Although bare carbon black surface and directional emitter samples have different solar reflectance, nano-PE-coated ones have nearly identical solar reflectance at the same solar

Please cite this article in press as: Zhou et al., Angle-selective thermal emitter for directional radiative cooling and heating, Joule (2023), https://doi.org/10.1016/j.joule.2023.10.013

incidence angle (Figures S11 and S12). This ensures that the temperature difference between these samples is mostly governed by their radiative properties. We also note that, although the top nano-PE layer will decrease the emissivity in the near-IR range due to its increased reflectance, its high transmittance in the mid-infrared range ensures that the angle-dependent emissivity of the directional emitter in the 8–13 μm range is preserved (Figure S13), which is critical for radiative cooling application. Environmental stability of the nano-PE material has also been characterized, and nano-PE was found to be generally stable against a series of durability tests mimicking outdoor conditions (see details in Notes S1–S6 and Figures S14 and S15). For outdoor experiments, all samples are placed on foam insulations and enclosed in a box covered with aluminum mylar sheets.

We first place all samples horizontally such that they all face the sky and solar irradiation. In such case, the carbon black paints should achieve the lowest temperature due to their largest radiative cooling power to the sky, as demonstrated in Figure 3A. This is followed by the directional emitter that radiatively cools itself down via directional thermal emission to the sky. The aluminum mylar film has the highest temperature because it has negligible radiative cooling power due to low hemispherical emissivity. Next, we install samples vertically to the ground. In this configuration, samples face the sky and the hot ground for its upper half and lower half of the hemisphere above the sample surfaces, respectively. Both the carbon black paints and the directional emitter radiatively cool efficiently by their large emissivity toward the sky. The directional emitter cools down further by reflecting the thermal radiation from the ground, whereas the carbon black absorbs significant heat by radiation from the ground. Therefore, the directional emitter achieves the lowest temperature. We note that the large temperature difference between the low-emissivity material and two other cases is also partly due to the slightly smaller solar reflectivity of aluminum mylar compared with that of nano-porous PE (Figure S12). When we turn all samples away from sunlight, the temperatures of the aluminum mylar film and the carbon black paints decrease and reach similar temperatures. This indicates that cooling of the carbon black paints by thermal radiation to the sky is largely offset by heating due to thermal radiation from the ground. Still, the directional emitter has the best cooling performance and reaches temperatures about 2°C lower than other non-directional cases. To further eliminate the effects of solar heating, the above samples have also been tested in the nighttime where a hot plate with controlled temperature settings simulates the ground. Although the view factor between the sample and hot plate is small, significant temperature increases are observed for the carbon black paints when the hot plate temperature increases. By contrast, the directional emitter and aluminum mylar samples show small temperature changes, indicating that they can reject radiative heat flux from the hot plate (Figure S16).

We further conducted a full-day test with all samples installed vertically (Figure 3B). The samples face the west such that before noon there is no solar irradiation on the samples, whereas in the afternoon, the samples start to receive solar heat gain. Before sunrise, the carbon black paints and the directional emitter both reach sub-ambient temperature due to radiative cooling, whereas the aluminum mylar film stays around the ambient temperature. The temperature of the ground is also lower than the ambient due to its relatively high emissivity. After the sun rises, the ground temperature starts to increase. As the ground temperature becomes higher than the ambient temperature, the carbon black paints take additional heating penalty, and their temperature becomes increasingly higher compared with that of the directional emitter. Around noon, when the ground temperature reaches the maximum, the

Please cite this article in press as: Zhou et al., Angle-selective thermal emitter for directional radiative cooling and heating, Joule (2023), https://doi.org/10.1016/j.joule.2023.10.013

carbon black is at even higher temperatures than the aluminum mylar film, which highlights the significant heating due to the thermal radiation from the ground. Throughout the day, the directional emitter achieves the lowest temperature among all samples, demonstrating the advantage of directional emissivity in cooling energy saving.

To assess the practical impact of directional emitter materials on building energy efficiency, we conducted energy-saving simulations using a standard reference model,[29] specifically a post-1980 midrise apartment building. Our analysis primarily focuses on heat transfer through building walls, where the net heat influx, combined with internal heat generation, determines the overall cooling demand (see details in Notes S1–S6 and Figure S17). The application of directional emitter materials to the exterior surface of building walls effectively alters their emissivity and absorptivity characteristics. This strategy offers the most substantial benefits in hot climate zones, where buildings typically have lower insulation levels. In these areas, we observed a cooling energy reduction of up to 40% (Figure 3C). Nevertheless, even in regions with well-insulated buildings, we anticipate cooling energy savings of 10%–20%. Across the United States, the incorporation of directional emitters into building walls has the potential to reduce cooling loads by 10%–40%, leading to significant energy and emission reductions (Figure 3D). We recognize that energy-saving benefits vary worldwide depending on specific climate conditions. For instance, radiative cooling is less effective in humid areas,[30] making the benefits of a directional emitter less pronounced. In such environments, a low-emissivity material that rejects ambient heat might be a more suitable choice. Broadly speaking, for outdoor cooling, directionally emitting surfaces offer the greatest energy-saving potential in hot, arid conditions.

Directional radiative heating

Due to the confined angular range of high emissivity, angle-selective emitters can emit heat radiation to a target that requires heating while minimizing radiation to other unwanted directions, thereby reducing heating energy consumption. To demonstrate such capability of a directional emitter, we fabricated a ring-shaped emitter (Figure 4A). The directional emitters with the narrowest angular range of emission (sample 4) are placed on a copper ring heater with their wedges facing the center of the ring. Another heater painted with carbon black is used as an isotropic blackbody reference. To visualize the radiation profiles, we built a setup to capture heat radiation and turn it into temperature profiles (Figure 4B). We placed a thin carbon-painted PE film in front of the emitter. Heat radiation is absorbed by the film and leads to local temperature increases. An infrared camera from the back then captures the temperature distribution, which indicates the radiation profiles of the emitter. Figures 4C and 4D compare the captured infrared images from the isotropic and directional emitters. For the blackbody emitter, the heat radiation goes in all directions (Figure S18), leading to a ring-shaped heating pattern (Figure 4C). By contrast, for the directional emitter, because of the wedge orientations, the emissivity is only large when the emission direction is pointing toward the center (Figure S18). Consequently, most radiative heat fluxes go toward the center where maximal temperature increase is observed (Figure 4D). We note this contrast in heating pattern is not due to view factor, which is a geometric factor describing the radiative heat exchange between surfaces, but instead is a result of the different angular emission property of the emitter surface. The ring-shaped heater has been chosen to illustrate the capability of directional emitters to emit heat radiation to a localized region. Similar examples can also be given by planar heaters. Although a single planar heater with our directional emitter design would only allow radiation into a

Please cite this article in press as: Zhou et al., Angle-selective thermal emitter for directional radiative cooling and heating, Joule (2023), https://doi.org/10.1016/j.joule.2023.10.013

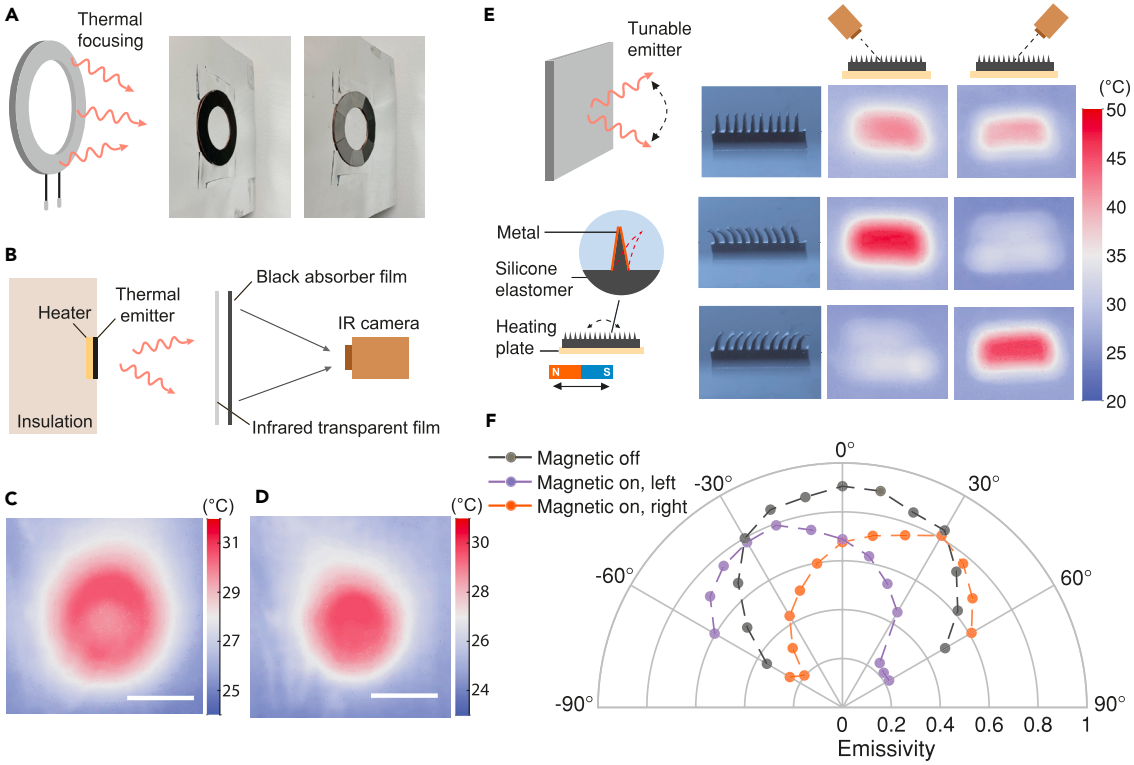

Figure 4. Directional radiant heating and magnetic steering

(A) Schematic and photo of ring-shape heat emitter.

(B) Measurement setup to capture thermal radiation and turn into temperature profiles that are visualized using an infrared camera.

(C and D) Captured temperature profiles indicating the radiation profiles from a black emitter (C) and a directional emitter (D). The scale bars represent 5 cm.

(E) Schematic and photos showing magnetic control of thermal emission direction. The micro-wedge has two sides coated with metal and can bend toward different directions depending on the magnetic field direction.

(F) Angle dependence of apparent emissivity values under magnetic control.

skewed direction (see Figure S18), two planar directional emitter heaters pieced together can also deliver heat to a laterally focused region (Figure S19). In principle, the wedge orientations can also be spatially inhomogeneous such that the radiative heating range can be further optimized.

The capability of delivering heat radiation to a local region brings energy-saving potential for heating applications. The radiant heating flux is governed by the emitter temperature and surface emissivity. For a remote target, a directional emitter can deliver the same heat radiation as a blackbody emitter if the target is located within the high-emissivity angular range of the directional emitter and the emitters are at the same temperatures. In such case, however, the blackbody emitter consumes more energy as it emits radiation to all directions. For example, the ring-shaped directional emitter in general requires 20% less heating power compared with the blackbody emitter when the emitters are heated to the same temperature set points (Figure S20). Therefore, if the same heating power is supplied, the directional emitter would have higher temperature due to its smaller radiative heat loss. Consequently, the directional emitter heats up a target more efficiently than the blackbody emitter because of the ability to focus heat radiation and minimize radiative heat loss to unwanted regions (Figure S20). An additional benefit of our design is that the thermal emission directionality is achieved through introducing a microstructure on the

Please cite this article in press as: Zhou et al., Angle-selective thermal emitter for directional radiative cooling and heating, Joule (2023), https://doi.org/10.1016/j.joule.2023.10.013

material surface. This allows the development of a wallpaper-like material with tailored heat radiation direction, which makes practical installation convenient (e.g., as a retrofit to existing radiant heaters). Although the proof-of-concept demonstrations mentioned above are conducted on a centimeter scale, it is feasible to scale up heat delivery to a meter scale by proportionally increasing the dimensions of the radiant heater. Our ray tracing simulation reveals that by implementing planar radiators equipped with directional emitters measuring 50 cm laterally, we can efficiently radiate heat to a local area located 3 m away from the radiator while significantly decreasing overall radiative heat loss (Figure S21). This result demonstrates the practical potential of directional emitter materials for residential heating applications.

Magnetically tunable directional emitter

The above concept of directional radiative cooling and heating can be further extended to direction-tunable thermal emitters, opening up possibilities for dynamic control of thermal radiation. The strategy is to create microstructures that are responsive to external stimuli and can deform such that strong absorption of radiation would occur at different incidence angles. To demonstrate this, we created a vertically aligned micro-wedge structure that dynamically changes wedge angles by magnetic force exerted on the embedded iron microparticles through an external magnetic field. Iron as a soft magnetic material makes the structure responsive to magnetic fields.[31] The side walls of the wedges are coated with metal (Figure 4E). Figure 4E shows that under different field directions, the vertically aligned wedges deform in different directions. Radiative heat flux coming from the direction facing the deformed wedges would be absorbed, leading to high emissivity. Radiative heat flux coming from the other direction is instead mostly reflected, giving rise to low emissivity. Altering the wedge orientation thereby changes the direction of thermal emission, as shown by the infrared images taken at different viewing angles (Figure 4E). Angle-dependent apparent emissivity values can be extracted from the infrared images and are shown in Figure 4F, demonstrating a magnetically controlled, direction-tunable thermal emitter material.

DISCUSSION

Engineering of directional emissivity opens up a new opportunity of thermal emission control that can tailor radiative energy exchange to match and harness the largely inhomogeneous temperature in the environments to achieve energy-efficient cooling and heating. The fabrication of our micro-structured directional thermal emitter is based on a mold-casting process, which is similar to the approach used to fabricate various industrial products. Alternatively, one may also explore other fabrication methods such as screen printing or engraving to fabricate such microstructures so that the process is applicable to large-scale applications in the building and industry sectors. Silicone elastomer as the main material makes the structure flexible and stretchable, which can conform to various geometries. The material's thinness and flexibility provide a user-friendly, wallpaper-like installation convenience. The concept can also be generalized to other material systems, various structures, and even dynamic control with other external stimuli. The potential for direction-tunable thermal emissivity further opens the door to dynamically directing radiative energy toward moving targets, particularly in indoor heating scenarios. We believe further research on directional control of thermal radiation holds great potential in achieving energy saving for a variety of applications spanning from space cooling and heating to waste heat recovery[32] and solar thermal power generation.

Please cite this article in press as: Zhou et al., Angle-selective thermal emitter for directional radiative cooling and heating, Joule (2023), https://doi.org/10.1016/j.joule.2023.10.013

EXPERIMENTAL PROCEDURES

Resource availability

Lead contact

Further information and requests for resources and materials should be directed to the lead contact, Yi Cui (yicui@stanford.edu).

Material availability

The materials in this study will be made available upon reasonable request.

Data and code availability

All data are present in the paper and supplemental information.

Materials

To manufacture the wedge-shaped emitter material, a mold is first created using a hybrid process of orthogonal cutting and wedge indenting.[27] A soft wax mold is first planed using an end mill and then using a sharp microtome blade (~1 μm tip radius). Using the same microtome blade following an oblique trajectory, a series of indentations is made on the surface of the wax mold to create wedge-shaped cavities on the order of 100 μm. The angle, width, depth, and spacing of these wedges can be controlled by adjusting the tool geometry and the machining path, such as the tool's indenting angle and retracting angle. A two-part silicone (SYLGARD, 184) is poured into the mold to create the bulk material with these micro-wedge structures. The surface of the structure is further plasma cleaned before final aluminum metal deposition (150-nm thickness). Although preparing the wax mold requires creating the wedges one by one, once the mold is created, it can be repeatedly used to fabricate silicone material with microstructures.

To manufacture the vertically aligned micro-wedge emitter with magnetic response, we first create an acrylic mold by cutting out grooves (width about 50–100 μm) using a laser cutter. A two-part silicone (Ecoflex, 00-10) is then mixed with iron microparticles (Sigma Aldrich #267953, 25 wt %) and cast into the mold to form a continuous silicone-iron elastomer composite. The sample is then deposited with gold (100 nm) in an evaporator at a tilted angle such that the metal deposition mainly occurs on the side walls of the wedges but not at the bottom. Depositions are made twice to coat the two sides of the wedges.

To make nano-porous PE (nano-PE) film, high-density PE and ultrahigh molecular weight PE are first mixed with paraffin oil (in a weight ratio of 1:4:35) at about 190°C under stirring. The mixed solution is then cast onto a heated substrate at about 170°C. After cooling down, the solidified film is peeled off from the substrate. Methylene chloride is then used to extract paraffin oil from the material, and a nano-PE film is created after drying.

Electromagnetic wave simulation

Electromagnetic wave simulation was carried out to study the absorption profiles of the structure at different incidence angles. The wavelength of the incoming wave is fixed at 10 μm. The structure is made of silicone elastomer (complex refractive index of 1.8 + i0.154) and 100 nm thick aluminum metal (complex refractive index of 25 + i85.96), following the geometry of the manufactured samples. Periodic boundary condition is used in the direction of repeating units. The incident power density is 1 W/m. Under incident radiation at an angle θ from the normal to the surface, total reflectivity R is calculated by evaluating the ratio of the incident power to the time-averaged power flow leaving the top domain boundary. Results from transverse

Please cite this article in press as: Zhou et al., Angle-selective thermal emitter for directional radiative cooling and heating, Joule (2023), https://doi.org/10.1016/j.joule.2023.10.013

electric polarization and transverse magnetic polarization are averaged. Directional emissivity $\varepsilon(\theta)$ is calculated by $\varepsilon(\theta) = 1 - R$. Geometric dimensions of wedge structures corresponding to different tilting angles are given in Table S1.

Angle-dependent infrared absorption spectrum

Fourier transform infrared spectrometer with an integrating sphere is used to measure the total reflectance of the sample at different orientations. The sample is placed on a rotation holder at the opening port of the integrating sphere, and the orientation of the sample is adjusted by rotating the holder (Figure S2). The sample holder and its supporting structure (Figure S2) are covered with aluminum foil to ensure that diffuse reflections do not leave from the inner space of the integrating sphere. The infrared beams are focused to the center of the opening port and take up a small area, whereas the sample size occupies a significant area of the opening port. This ensures most of the infrared light is incident on the sample. The sample holder has also been validated against reference samples, including carbon black paint and aluminum mylar (Figure S6), showing angle-independent emissivity consistent with the optical properties of these reference materials. Baseline reflectance measurements were conducted using a gold reference sample. As our samples are optically thick, the measured reflectivity R can be directly converted to absorptivity $\alpha(\theta)$ at an incident angle of the beam θ, which is equivalently the emissivity $\varepsilon(\theta)$ at a given wavelength ($\varepsilon(\theta) = \alpha(\theta) = 1 - R$).

Environmental durability test

To understand the environmental durability of the material with respect to the proposed case demonstrations, we have performed durability tests for both directional emitter material and nano-PE material. These tests include UV stability test, high-temperature test, water flushing test, and abrasion resistance test. For UV stability test, the test material is illuminated by a 220 W UV light-emitting diode (LED) lamp continuously for 1 week. For high-temperature test, the test material is placed in an oven at a temperature of 70°C for 1 week. For the water flushing test, the test material is fixed with a tilting angle of 45° at 5 cm from a water faucet. Water continuously flows over the material for 1 week, and the flow rate is 300 mL/min. For abrasion resistance test, the test material with an area of 3 cm^2 is fixed on a glass slide and placed on sandpaper (grit size 400) facing downward. A 50 g weight is placed on the glass slide. The slide is moved on sandpaper for 10 cm to examine the material's abrasion resistance.

Cooling energy-saving simulation

Building energy-saving simulation is conducted using a reference building model (post-1980 midrise apartment) defined by US Department of Energy[29] across 200 cities in the United States. This model assesses the potential energy savings achievable through directional emitter materials by examining heat transfer through building walls. In brief, we examine a steady-state scenario where the combined heat influx into the building and internal heat generation must be managed by air conditioning, defining the total cooling load. The indoor temperature is set to be 22°C, whereas the outdoor temperatures are obtained from TMY3 weather data. We consider two cases—buildings with conventional wall materials and buildings with directional emitters covering their walls. The difference in the cooling load between these two scenarios quantifies the energy savings. For conventional buildings, surface emissivity/absorptivity properties are derived from EnergyPlus models.[33] For buildings with directional emitters installed on their wall surfaces, emissivity/absorptivity properties are taken from our measurement data. The effect of precipitable water vapor in the atmosphere significantly impacts the radiative cooling capacity[34] and is taken into account in the estimation of the sky emissivity based on the dew point following

Please cite this article in press as: Zhou et al., Angle-selective thermal emitter for directional radiative cooling and heating, Joule (2023), https://doi.org/10.1016/j.joule.2023.10.013

EnergyPlus models. Additionally, we assume an internal heat load of 10 W/m^2 (based on floor area) to represent average heat gain throughout the day.[35] Further simulation details can be found in the supplemental information.

Outdoor radiative test

For the outdoor test, all samples (dimension: 4 cm by 4 cm) are placed on foam insulations and enclosed in acrylic boxes covered with aluminum mylar. The aluminum mylar helps to minimize solar heat gain from radiation absorbed by the box surfaces. The opening above the samples is covered with PE films (thickness: 20 μm) to allow radiative heat exchange while minimizing convective heat loss. Thermocouples are attached to the backside of the samples to monitor the samples' temperatures. The measurement setups are placed on a rooftop of a three-story building in Stanford, California where the place is covered with particles of sand and pebbles, reasonably mimicking ground conditions with a relatively high emissivity. The temperature of this ground is measured by placing a thermocouple under the sand particles. The ambient temperature is recorded by the weather station located on the rooftop, and the solar irradiance is measured by a pyranometer installed near the samples.

Directional radiant heating

A ring-shaped heater with an outer diameter of 8 cm and an inner diameter of 4.5 cm is used to demonstrate directional radiant heating. The heater is made of copper (for good heat spreading), whose backside is attached with thin polyimide heaters, and its frontside is covered with emitter materials to be tested. A thermocouple is also attached to the backside of the copper heater for monitoring and controlling the temperature of the heater. The heater is placed on foam insulations covered with aluminum mylar, such that only the heater area will emit radiation, whereas other regions would have negligible emission. A carbon-coated PE film receives heat radiation from the emitter and leads to local temperature increases, which are captured from the backside with an infrared camera. A transparent PE film is placed before the black film to allow infrared radiation to pass through while minimizing the convective heat loss that disturbs the temperature distributions. For radiative heater at a set temperature point, the heating power supplied to the heater is calculated by multiplying the voltage with the current that runs through the polyimide heater.

Apparent emissivity from infrared images

The infrared camera measures the temperature by recording the infrared radiance within a certain bandwidth and converting that into temperature readings based on Planck's law. The sample emissivity in the camera setting can be changed but is set to one (blackbody) in our measurements. Based on Planck's law, the fourth power of the measured temperature T_{camera} is proportional to the total infrared emittance from the sample P: $P = \sigma T_{camera}^4$, where σ is the Stefan-Boltzmann constant. The actual total infrared emittance includes both direct emittance from the sample and reflectance from the surrounding environment, $P = \varepsilon\sigma T_{sample}^4 + (1-\varepsilon)\sigma T_{amb}^4$, where ε is the sample emissivity, T_{sample} the sample temperature, and T_{amb} the ambient temperature. With temperature reading from an infrared image, apparent emissivity values can then be obtained by $\varepsilon = (T_{camera}^4 - T_{amb}^4)/(T_{sample}^4 - T_{amb}^4)$ In the measurements of the magnetically tunable emitters, the magneto-optical responses of the magnetized iron particles under the external magnetic fields are negligible for infrared frequencies, and the apparent emissivity are not affected.

SUPPLEMENTAL INFORMATION

Supplemental information can be found online at https://doi.org/10.1016/j.joule.2023.10.013.

ACKNOWLEDGMENTS

Part of this work was performed at the Stanford Nano Shared Facilities (SNSF), supported by the National Science Foundation under award ECCS-2026822. S.F. acknowledges the support from the U.S. Department of Energy (grant no. DE-FG02-07ER46426). Y.C. acknowledges the support from the Future Investment Initiative Institute.

AUTHOR CONTRIBUTIONS

J.Z. and Y.C. conceived the project. J.Z., T.G.C., and A.H.-A. fabricated the microwedge structure. J.Z. and Y.T. performed the electromagnetic simulation for the absorption profiles. J.Z. conducted infrared absorption measurement, outdoor cooling test, energy-saving simulations, and directional radiative heating test, with help from L.F., Y.P., R.X., Y.W., and S.A. All authors commented on, discussed, and edited the manuscript.

DECLARATION OF INTERESTS

The authors declare no competing interests.

Received: March 27, 2023
Revised: May 15, 2023
Accepted: October 18, 2023
Published: November 8, 2023

REFERENCES

1. Lamb, W.F., Wiedmann, T., Pongratz, J., Andrew, R., Crippa, M., Olivier, J.G.J., Wiedenhofer, D., Mattioli, G., Al Khourdajie, A.A., House, J., et al. (2021). A review of trends and drivers of greenhouse gas emissions by sector from 1990 to 2018. Environ. Res. Lett. *16*, 73005. https://doi.org/10.1088/1748-9326/ABEE4E.

2. Peng, Y., and Cui, Y. (2020). Advanced textiles for personal thermal management and energy. Joule *4*, 724–742. https://doi.org/10.1016/J.JOULE.2020.02.011.

3. Jelle, B.P., Kalnæs, S.E., and Gao, T. (2015). Low-emissivity materials for building applications: a state-of-the-art review and future research perspectives. Energy Build. *96*, 329–356. https://doi.org/10.1016/J.ENBUILD.2015.03.024.

4. Yin, X., Yang, R., Tan, G., and Fan, S. (2020). Terrestrial radiative cooling: using the cold universe as a renewable and sustainable energy source. Science *370*, 786–791. https://doi.org/10.1126/SCIENCE.ABB0971.

5. Cui, Y., Ke, Y., Liu, C., Chen, Z., Wang, N., Zhang, L., Zhou, Y., Wang, S., Gao, Y., and Long, Y. (2018). Thermochromic VO_2 for energy-efficient smart windows. Joule *2*, 1707–1746. https://doi.org/10.1016/J.JOULE.2018.06.018.

6. Wang, S., Jiang, T., Meng, Y., Yang, R., Tan, G., and Long, Y. (2021). Scalable thermochromic smart windows with passive radiative cooling regulation. Science *374*, 1501–1504. https://doi.org/10.1126/SCIENCE.ABG0291.

7. Peng, Y., Fan, L., Jin, W., Ye, Y., Huang, Z., Zhai, S., Luo, X., Ma, Y., Tang, J., Zhou, J., et al. (2021). Coloured low-emissivity films for building envelopes for year-round energy savings. Nat. Sustain. *5*, 339–347. https://doi.org/10.1038/s41893-021-00836-x.

8. Fan, S. (2017). Thermal photonics and energy applications. Joule *1*, 264–273. https://doi.org/10.1016/J.JOULE.2017.07.012.

9. Raman, A.P., Anoma, M.A., Zhu, L., Rephaeli, E., and Fan, S. (2014). Passive radiative cooling below ambient air temperature under direct sunlight. Nature *515*, 540–544. https://doi.org/10.1038/nature13883.

10. Zhai, Y., Ma, Y., David, S.N., Zhao, D., Lou, R., Tan, G., Yang, R., and Yin, X. (2017). Scalable-manufactured randomized glass-polymer hybrid metamaterial for daytime radiative cooling. Science *355*, 1062–1066. https://doi.org/10.1126/SCIENCE.AAI7899.

11. Mandal, J., Fu, Y., Overvig, A.C., Jia, M., Sun, K., Shi, N.N., Zhou, H., Xiao, X., Yu, N., and Yang, Y. (2018). Hierarchically porous polymer coatings for highly efficient passive daytime radiative cooling. Science *362*, 315–319. https://doi.org/10.1126/SCIENCE.AAT9513.

12. Li, X., Peoples, J., Yao, P., and Ruan, X. (2021). Ultrawhite $BaSO_4$ paints and films for remarkable daytime subambient radiative cooling. ACS Appl. Mater. Interfaces *13*, 21733–21739. https://doi.org/10.1021/ACSAMI.1C02368.

13. Li, T., Zhai, Y., He, S., Gan, W., Wei, Z., Heidarinejad, M., Dalgo, D., Mi, R., Zhao, X., Song, J., et al. (2019). A radiative cooling structural material. Science *364*, 760–763. https://doi.org/10.1126/SCIENCE.AAU9101.

14. Tang, K., Dong, K., Li, J., Gordon, M.P., Reichertz, F.G., Kim, H., Rho, Y., Wang, Q., Lin, C.Y., Grigoropoulos, C.P., et al. (2021). Temperature-adaptive radiative coating for all-season household thermal regulation. Science *374*, 1504–1509. https://doi.org/10.1126/SCIENCE.ABF7136.

15. Bhatia, B., Leroy, A., Shen, Y., Zhao, L., Gianello, M., Li, D., Gu, T., Hu, J., Soljačić, M., and Wang, E.N. (2018). Passive directional sub-ambient daytime radiative cooling. Nat. Commun. *9*, 5001. https://doi.org/10.1038/s41467-018-07293-9.

16. Hsu, P.C., Song, A.Y., Catrysse, P.B., Liu, C., Peng, Y., Xie, J., Fan, S., and Cui, Y. (2016). Radiative human body cooling by nanoporous polyethylene textile. Science *353*, 1019–1023. https://doi.org/10.1126/SCIENCE.AAF5471.

17. Peng, Y., Chen, J., Song, A.Y., Catrysse, P.B., Hsu, P.C., Cai, L., Liu, B., Zhu, Y., Zhou, G., Wu, D.S., et al. (2018). Nanoporous polyethylene microfibres for large-scale radiative cooling fabric. Nat. Sustain. *1*, 105–112. https://doi.org/10.1038/s41893-018-0023-2.

18. Cai, L., Song, A.Y., Wu, P., Hsu, P.C., Peng, Y., Chen, J., Liu, C., Catrysse, P.B., Liu, Y., Yang, A., et al. (2017). Warming up human body by nanoporous metallized polyethylene textile. Nat. Commun. *8*, 496. https://doi.org/10.1038/s41467-017-00614-4.

19. Zhang, X.A., Yu, S., Xu, B., Li, M., Peng, Z., Wang, Y., Deng, S., Wu, X., Wu, Z., Ouyang, M., et al. (2019). Dynamic gating of infrared radiation in a textile. Science *363*, 619–623. https://doi.org/10.1126/SCIENCE.AAU1217.

20. Yang, R., and Yin, X. (2019). Passive cooling in an urban setting. Nat. Sustain. *2*, 663–664. https://doi.org/10.1038/s41893-019-0358-3.

21. Miriel, J., Serres, L., and Trombe, A. (2002). Radiant ceiling panel heating–cooling systems: experimental and simulated study of the performances, thermal comfort and energy consumptions. Appl. Therm. Eng. *22*, 1861–1873. https://doi.org/10.1016/S1359-4311(02)00087-X.

22. Hesketh, P.J., Zemel, J.N., and Gebhart, B. (1988). Polarized spectral emittance from periodic micromachined surfaces. I. Doped silicon: the normal direction. Phys. Rev. B Condens. Matter *37*, 10795–10802. https://doi.org/10.1103/PhysRevB.37.10795.

23. Greffet, J.J., Carminati, R., Joulain, K., Mulet, J.P., Mainguy, S., and Chen, Y. (2002). Coherent emission of light by thermal sources. Nature *416*, 61–64. https://doi.org/10.1038/416061a.

24. Chalabi, H., Alù, A., and Brongersma, M.L. (2016). Focused thermal emission from a nanostructured SiC surface. Phys. Rev. B *94*, 94307. https://doi.org/10.1103/PhysRevB.94.094307.

25. Xu, J., Mandal, J., and Raman, A.P. (2021). Broadband directional control of thermal emission. Science *372*, 393–397. https://doi.org/10.1126/SCIENCE.ABC5381.

26. Shen, Y., Hsu, C.W., Yeng, Y.X., Joannopoulos, J.D., and Soljačić, M. (2016). Broadband angular selectivity of light at the nanoscale: progress, applications, and outlook. Appl. Phys. Rev. *3*, 11103. https://doi.org/10.1063/1.4941257.

27. Day, P., Eason, E.V., Esparza, N., Christensen, D., and Cutkosky, M. (2013). Microwedge machining for the manufacture of directional dry adhesives. J. Micro Nano Manuf. *1*, 11001. https://doi.org/10.1115/1.4023161.

28. Cai, L., Song, A.Y., Li, W., Hsu, P.C., Lin, D., Catrysse, P.B., Liu, Y., Peng, Y., Chen, J., Wang, H., et al. (2018). Spectrally selective nanocomposite textile for outdoor personal cooling. Adv. Mater. *30*, e1802152. https://doi.org/10.1002/ADMA.201802152.

29. Deru, M., Field, K., Studer, D., Benne, K., Griffith, B., Torcellini, P., Liu, B., Halverson, M., Winiarski, D., Rosenberg, M., et al. (2011). U.S. Department of Energy commercial reference building models of the national building stock. Technical report NREL/TP-5500-46861 (National Renewable Energy Laboratory). https://www.nrel.gov/docs/fy11osti/46861.pdf.

30. Tso, C.Y., Chan, K.C., and Chao, C.Y.H. (2017). A field investigation of passive radiative cooling under Hong Kong's climate. Renew. Energy *106*, 52–61. https://doi.org/10.1016/j.renene.2017.01.018.

31. Kim, Y., and Zhao, X. (2022). Magnetic soft materials and robots. Chem. Rev. *122*, 5317–5364. https://doi.org/10.1021/ACS.CHEMREV.1C00481.

32. Davids, P.S., Kirsch, J., Starbuck, A., Jarecki, R., Shank, J., and Peters, D. (2020). Electrical power generation from moderate-temperature radiative thermal sources. Science *367*, 1341–1345. https://doi.org/10.1126/SCIENCE.ABA2089.

33. Crawley, D.B., Lawrie, L.K., Winkelmann, F.C., Buhl, W.F., Huang, Y.J., Pedersen, C.O., Strand, R.K., Liesen, R.J., Fisher, D.E., Witte, M.J., et al. (2001). EnergyPlus: creating a new-generation building energy simulation program. Energy Build. *33*, 319–331. https://doi.org/10.1016/S0378-7788(00)00114-6.

34. Zhao, D., Aili, A., Zhai, Y., Xu, S., Tan, G., Yin, X., and Yang, R. (2019). Radiative sky cooling: fundamental principles, materials, and applications. Appl. Phys. Rev. *6*, 21306. https://doi.org/10.1063/1.5087281.

35. Hendron, R., and Engebrecht, C. (2010). Building America research benchmark definition. Technical report NREL/TP-550-47246 (National Renewable Energy Laboratory). https://www.nrel.gov/docs/fy10osti/47246.pdf.